Environmental Science and Pollution Research (2023) 30:73849–73860
https://doi.org/10.1007/s11356-023-27589-8

RESEARCH ARTICLE

Responses of *Bacillus* sp. under Cu(II) stress in relation to extracellular polymeric substances and functional gene expression level

Ling-ling Wang[1] · Zheng-yan Yin[1] · Yun Xu[1] · Miao-yu Deng[1] · Kai-ming Zhang[1] · Quan Wang[1,2] · Rong-ping Chen[1] · Lei Yu[1,2]

Received: 19 December 2022 / Accepted: 8 May 2023 / Published online: 17 May 2023

Abstract

The production and composition of extracellular polymeric substances (EPS), as well as the EPS-related functional resistance genes and metabolic levels of *Bacillus* sp. under Cu(II) stress, were investigated. EPS production increased by 2.73 ± 0.29 times compared to the control when the strain was treated with 30 mg L^{-1} Cu(II). Specifically, the polysaccharide (PS) content in EPS increased by 2.26 ± 0.28 g CDW^{-1} and the PN/PS (protein/polysaccharide) ratio value increased by 3.18 ± 0.33 times under 30 mg L^{-1} Cu(II) compared to the control. The increased EPS secretion and higher PN/PS ratio in EPS strengthened the cells' ability to resist the toxic effect of Cu(II). Differential expression of functional genes under Cu(II) stress was revealed by Gene Ontology pathway enrichment analysis and Kyoto Encyclopedia of Genes and Genomes pathway enrichment analysis. The enriched genes were most obviously upregulated in the UMP biosynthesis pathway, the pyrimidine metabolism pathway, and the TCS metabolism pathway. This indicates an enhancement of EPS regulation-related metabolic levels and their role as a defense mechanism for cells to adapt to Cu(II) stress. Additionally, seven copper resistance genes were upregulated while three were downregulated. The upregulated genes were related to the heavy metal resistance, while downregulated genes were related to cell differentiation, indicating that the strain had initiated an obvious resistance to Cu(II) despite its severe cell toxicity. These results provided a basis for promoting EPS-regulated associated functional genes and the application of gene-regulated bacteria in heavy metal-containing wastewater treatment.

Keywords Extracellular polymeric substances (EPS) · *Bacillus* sp. · Heavy metal-resistant · Resistance gene

Introduction

Heavy metal pollution has the characteristics of non-degradability, bioaccumulation, and toxicity sustainability (Weber et al. 2001). Once ingested, they are hardly removed by excretion, which makes them easily enriched in organisms continuously through the food chain (Ayangbenro et al. 2019). Hence, even a tiny dose of heavy metals poses a great threat to human body and ecological environment (Chowdhury et al. 2016). Copper is one of the most common heavy metals with extensive biological toxicity. It was reported that exposing microorganisms to solid copper surface would increase the mutation rate or DNA damage (Espirito Santo et al. 2011). Therefore, discharging copper-containing wastewater into water bodies greatly reduces the self-purification capacity of the water and brings great pressure to the balance of the aquatic ecosystem (Vale et al. 2016). At present, the treatment technologies for heavy metal-containing wastewater include reverse osmosis, ion exchange, chemical deposition, electrochemical treatment, electrodialysis, membrane filtration, and flocculation adsorption (Vasudevan and Oturan 2013; Jamshidifard et al. 2019). Among them, flocculation adsorption is widely used, but the added chemical reagent can become a secondary pollutant (Xu et al. 2018). To solve this dilemma, bioflocculation, which does not incur the risk of secondary pollution, was investigated (Hashim et al. 2011). The core of bioflocculation is bioflocculants

Responsible Editor: Diane Purchase

✉ Lei Yu
lyu@njfu.edu.cn

[1] Department of Environmental Engineering, College of Biology and the Environment, Nanjing Forestry University, Nanjing 210037, China

[2] College of Biology and the Environment, Co-Innovation Center for Sustainable Forestry in Southern China, Nanjing Forestry University, Nanjing 210037, China

such as chitosan extracted from shellfish or fish by-products (Ola et al. 2023) and extracellular polymeric substances (EPS) secreted by microorganisms (bacteria, fungi, algae) (Mohd Nasir et al. 2019).

EPS could be secreted in situ, which means less cost and excellent solubility compared to chitosan, making it more suitable for application in wastewater treatment. EPS are natural organic compounds secreted by cells, and the main components are polysaccharides, proteins, nucleic acid, and humus (Li et al. 2021). EPS were investigated as a potential alternative to chemical flocculation due to their environment-friendly advantages (Hua et al. 2021). Despite these merits, heavy metals can be universally toxic to living cells, leading to cell death (Lian et al. 2022). Additionally, the preparation of EPS before use increases the cost in engineering applications. The solution to this predicament is to promote in situ EPS secretion, which can serve as a bioflocculant in wastewater treatment. It has been noted that when cells are exposed to adverse environments, i.e., heavy metals, EPS secretion is stimulated, which can serve as a self-defense mechanisms (Van Acker et al. 2014; Holmes et al. 2016) (Yu 2020). This defense mechanism could solve the dilemma that EPS must be preprepared before use, making it possible to apply in situ produced EPS directly to heavy metal wastewater treatment. Moreover, the stimulation of more EPS can act as a bioflocculant to improve heavy metal removal efficiency.

Research on the EPS self-defense mechanism can be summarized as follows. (1) Reasons why microorganisms tend to produce EPS under adverse conditions: EPS can serve as a permeation barrier and reducing reactant. For example, EPS wrapping around *E. coil* cells was secreted to decrease the toxicity of Ag^+ (Kang et al. 2017), and EPS of *Acidithiobacillus ferrooxidans* strain serve as an electron donor in iron tailings treatment (Yi et al. 2021). (2) Quantity analysis of EPS secretion response: in general, it is well known that EPS secretion increases under low concentrations of heavy metal stress. EPS production increased by 8% when dosing 0.75 mg L^{-1} nZnO (Ma et al. 2022) (3) Evaluation of functional genes for EPS secretion: EPS secretion was stimulated under the stress of triclosan for the increased expression of four functional genes *IntI1*, *sul1*, *mexB*, and *tnpA* (Zhao et al. 2022). In conclusion, current studies about the self-defense mechanisms are limited to the mechanisms of how heavy metals affect EPS secretion. It is unclear whether it can initiate the self-protection mechanism of EPS secretion in situ when treating heavy metal wastewater. If it does exist, further exploration of the EPS-regulated functional resistance genes under copper stress is expected.

The main objective of this study is to compare the differences in EPS secretion previously studied for *Bacillus* (Zheng et al. 2008; Fang et al. 2011) and to investigate the changes in functional resistance gene expression and metabolic levels under Cu(II) stress. This work aims to provide more insights into the expression of unknown genes and broaden the possible mechanisms of EPS regulation. *Bacillus* sp. (CICC 23870) was used as the model strain to study the response of EPS secretion under different stress of simulated copper-containing wastewater. The cell growth, Cu(II) removal efficiency, and the EPS secretion would be analyzed through batch experiments and chemical assays. An array of spectroscopic technologies including FTIR, 3D-EEM, and XPS was used to analyze the variations in functional groups, active components, and elements involved in the reactions. Transcriptome gene sequencing was employed to determine the regulation of resistance genes under Cu(II) stress, and GO and KEGG pathway enrichment analyses were used to analyze the specific metabolic level changes. This study provided valuable insight into the possible self-defense mechanism of EPS regulation under Cu(II) stress, providing technical guidance and theoretical support for the biological treatment of heavy metal wastewater.

Methods and materials

Chemicals

The polysaccharide fluorescent dye, Calcofluor white stain, was purchased from Sigma-Aldrich. LIVE/DEAD™ BacLight™ bacterial viability kit (L13152) was bought from Thermo Fisher. Tryptone and yeast extract were obtained from OXOID. All other analytical chemicals including $CuSO_4$ were purchased from Sinopharm Chemical Reagent, China.

Strain and culture medium

In this study, strain *Bacillus* sp. (CICC 23870) was used as the model EPS-producing strain. Liquid Luria-Bertani (LB) medium (g L^{-1}) (Tryptone, 10; yeast extract, 5; NaCl, 10; pH,7.2) was used for aerobic cultivation of *Bacillus* sp. cells. The main constituents of EPS fermentation medium contain the following (g L^{-1}): glucose, 20; yeast extract, 2.0; urea, 1.0; KH_2PO_4, 2.0; K_2HPO_4, 2.0; $MgSO_4{\cdot}7H_2O$, 0.1 and 1% of SL-6 trace element solution. The SL-6 solution includes (mg L^{-1}) $ZnSO_4{\cdot}7H_2O$, 100; $MnCl_2{\cdot}4H_2O$, 30; boric acid, 300; $CoCl_2{\cdot}6H_2O$, 200; $CuCl_2{\cdot}2H_2O$, 10; $NiCl_2{\cdot}6H_2O$, 20; and $Na_2MoO_4{\cdot}2H_2O$, 30. The culture medium must be sterilized before using, and the carbon source and $MgSO_4$ solutions were autoclaved separately then combined aseptically before using.

EPS extraction

The *Bacillus* sp. cells were aerobically cultured in 100 mL of LB medium at 37°C for 12 h to reach the stationary phase. The cells ($OD_{660} \approx 1.5$) were separated from the medium by centrifugation (8000*g* at 4 °C for 10 min) and then resuspended in phosphate buffer solutions (PBS). The mixture was transferred into 98 mL of fresh, sterilized EPS fermentation medium with a 2% inoculation rate under different initial Cu(II) concentrations (0, 10, and 30 mg L^{-1}). The cells were recultured to reach the stationary phase and were used for EPS extraction using the sonication and alkali treatment method (Hua et al. 2021). Briefly, the pH value of the broth was adjusted to 12.5 and then subjected to ultrasonic treatment for 10 min. Then, the broth was centrifuged (8000*g*, 4°C, 15min) and the supernatant was poured into twice the volume of ice-cold alcohol. The mixture was settled at 4 °C for 48 hours to obtain the precipitation, which was dissolved in deionized water and then dialyzed for 24 h at 4 °C (Zhang et al. 2021b). Finally, the cotton-like white cluster EPS were obtained after lyophilization.

Analytical methods

Cell growth was monitored by measuring the optical density (OD) at 660 nm using a UV-vis spectrophotometer (UV-2550, Shimadzu, Japan). Liquid samples were collected from the fermentation broth at predetermined time intervals to determine the Cu(II) removal efficiency. The samples were then centrifuged at 8000*g* for 10 min, and the supernatant was filtered through a 0.22 μm hydrophilic polytetrafluoroethylene membrane. The obtained filtrate was used to determine the Cu(II) concentration using atomic absorption spectrometry (TAS-990, Puxi, China).

The EPS surrounding the cell surface before and after EPS extraction were stained by Calcofluor white stain (Wang et al. 2021). In short, the cell pellets before and after EPS extraction were transferred (1.5 μL) to a slide. Then, a drop of Calcofluor white stain and KOH solution (10%, w/v) were added and settled for 20 min; afterwards, excess dyes were washed with sterile water. The stained samples were then observed using a fluorescence microscope (BX53, Olympus) with a fluorescent CCD camera (DP73, Olympus). The bacterial viability before and after EPS extraction was detected by the LIVE/DEAD™ BacLight™ bacterial viability kit according to the manufacturer's instructions. The ratios of live and dead cells were estimated using ImageJ software. The protein and polysaccharide contents in EPS were measured using the Bradford assay method and Anthrone reagent method, respectively. The dried EPS powder was mixed and grinded with KBr (1:150) and then treated using tablet pressing method (Hua et al. 2021). The functional groups in EPS were detected in a FTIR spectrometer (Bruker VERTEX 80 V) with a spectral range of 4000−400 cm^{-1}. The element composition of EPS was determined using XPS spectrometer (AXIS Ultra DLD, Shimadzu, Japan). The fluorescence intensity of the EPS samples was analyzed using a 3D-EEM fluorescence spectrometry (LS-55, PerkinElmer, USA) with an excitation wavelength range of 200−450 nm and an emission wavelength range of 250−550 nm.

Functional gene change detection

Transcriptome sequencing was used to analyze changes in related resistance genes and metabolic levels among *Bacillus* sp. cultured under 10 mg L^{-1} Cu(II) in contrast to the normal culture conditions. Initially, total RNA was extracted and agar gel electrophoresis was used to detect the integrity and purity. The qualified RNA (RIN > 7) was then isolated using a rRNA removal kit and broken into 200–300 bp fragments by ion disruption (Ola et al. 2023). Random primers and reverse transcriptase were used to synthesize cDNA, and a library was constructed with a size of 300–400 bp (Meis and Khanna 2009). After library construction, quality inspection was carried out using an Agilent 2100 Bioanalyzer and the sequencing was performed on the Illumina platform. The sequencing results were compared and annotated with reference genes. Finally, differential gene cluster analysis and GO and KEGG pathway enrichment analysis were used to analyze differentially expressed genes and changes in metabolic levels.

Results and discussion

Adsorption of Cu(II) onto cell and its toxic effect on cell growth

The cells obtained after aerobic cultivation in LB medium were inoculated into a copper containing (0, 10, and 30 mg L^{-1} of Cu(II)) fermentation medium. As shown in Fig. 1A, the maximum OD_{660} value (3.56 ± 0.23) for cell growth was reached in the control experiment after 48 h, while the OD_{660} values for batch experiments with Cu(II) were significantly lower, especially at 30 mg L^{-1} of Cu(II). And the cell growth was completely inhibited under 50 mg L^{-1} of Cu(II), as shown in Fig. S2. These results suggested that the strain *Bacillus* sp. can only adapt to stress of Cu(II) lower than 30 mg L^{-1} and then 10 and 30 mg L^{-1} chosen as appropriate mild and high stress levels for further research on EPS secretion. However, 30 mg L^{-1} of Cu(II) resulted in cell death and severe RNA degradation, making it unsuitable for gene sequencing. Therefore, 10 mg L^{-1} of Cu(II) was chosen as the suitable stress level for investigating the regulation of functional genes and metabolic levels. The cell growth curve under Cu(II) was similar to that in the presence

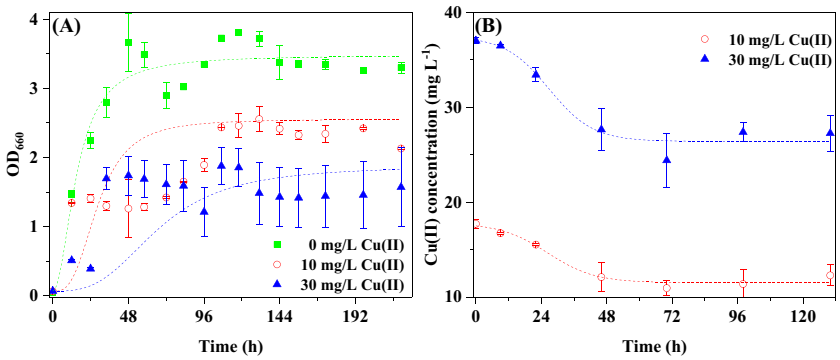

Fig. 1 Aerobic growth of *Bacillus* sp. under difference Cu(II) concentration (**A**) and Cu(II) concentration versus incubation time (**B**)

of *n*-BuOH (Xia et al. 2016), indicating that higher stress concentration resulted in stronger inhibition of cell growth. Interestingly, Cu(II) ions were gradually removed as the cells grew (Fig. 1B), with removal efficiencies of 38.5 ± 1.14% and 34.04 ± 1.46% for 10 mg L^{-1} and 30 mg L^{-1} of Cu(II), respectively. This suggested that higher concentrations of Cu(II) resulted in better removal effects, possibly because copper ions can enter the cells and be removed from the medium. Moreover, the dead cells, along with the secreted EPS, could serve as an adsorbent for copper ions (He et al. 2021). Based on these findings, EPS secretion under Cu(II) stress would be compared as follows.

EPS variation in the presence of Cu(II)

As showed in Fig. 2A, more EPS were secreted with a significant increase in Cu(II) concentration. EPS concentrations (g CDW^{-1}) were measured to evaluate the changes in EPS secreted by a single dry cell, and the exchange formula between cell dry weight (CDW) and the OD_{660} value was 1.0 OD_{660} ≈ 170.43 μg CDW ml^{-1} (Yu et al. 2020). The total extracted EPS concentration in the control (0 mg L^{-1}) was 3.48 ± 0.19 g CDW^{-1}, while that extracted under 10 and 30 mg L^{-1} of Cu(II) was 11.38 ± 0.57 g CDW^{-1} and 12.95 ± 0.72 g CDW^{-1}, respectively. EPS secretion was stimulated and increased the most (9.47 ± 0.65 g CDW^{-1}) despite severe inhibition of cell growth under 30 mg L^{-1} of Cu(II) (Fig. 1A). This illustrated that heavy metals, i.e., copper, can trigger bacteria to produce more EPS as a self-defense mechanism (Fu et al. 2022). Interestingly, EPS production was the highest at 30 mg L^{-1} Cu(II) stress in Fig. 2A, and the adsorption effect was the best at the same concentration in Fig. 2B. Furthermore, Cu(II) removal efficiency showed a positive correlation with initial Cu(II) concentrations, which may be because the EPS secreted under 30 mg L^{-1} of Cu(II) has stronger adsorption capacity and can absorb more copper ions efficiently compared to that secreted under 10 mg L^{-1} of Cu(II) (Li et al. 2020; Li et al. 2022). This demonstrated that more EPS secretion stimulated by copper ions can further increase the removal capacity for copper ions (Fang et al. 2022b).

As exhibited in Fig. 2B, the main components in extracted EPS (PS and PN) were analyzed (Bai et al. 2022). The increased secretion of EPS was mainly caused by the rising

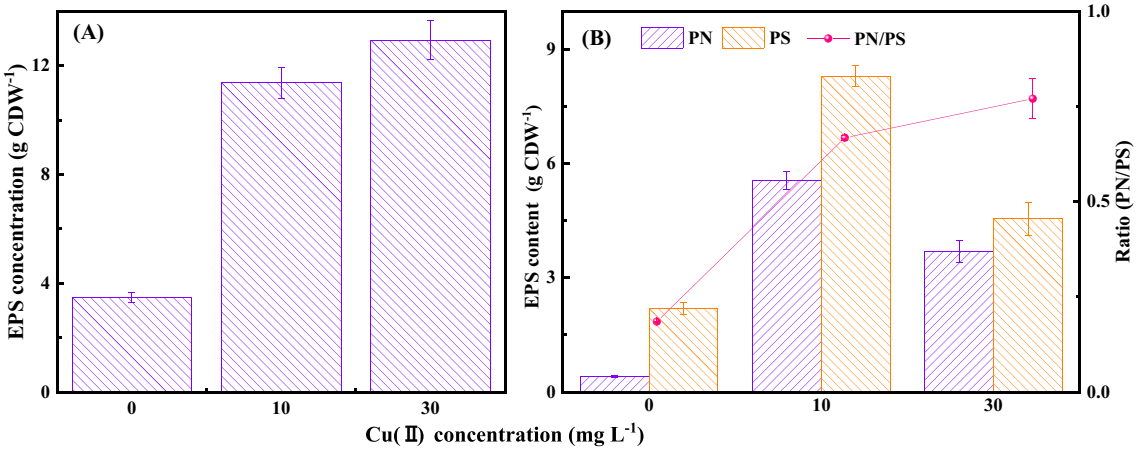

Fig. 2 Effect of Cu(II) with different initial concentration (0, 10, and 30 mg L^{-1}) on the production of EPS (**A**), and the variations of protein and polysaccharide component concentrations in EPS (**B**)

PS content, which increased from 2.20 ± 0.16 g CDW^{-1} to 4.55 ± 0.43 g CDW^{-1} as the Cu(II) concentration increased from 0 to 30 mg L^{-1}. Cu(II) stress overwhelmingly stimulated the secretion of PS over PN, indicating that the bacteria could secrete more PS as a resistance response mechanism, probably due to the fact that PS can act as a stable permeation barrier due to its thermodynamic stability and superior dispersibility compared with PN (Dong et al. 2022). The PN/PS ratio values showed a step-by-step increase with the increase in Cu(II) concentration from 0 to 30 mg L^{-1}. The increased PN/PS ratio suggested an improvement in the hydrophobicity of anammox granules (Chen et al. 2019), thereby improving cell aggregation and acting as a coping strategy to relieve copper stress (Tang et al. 2021; Fu et al. 2022). Additionally, it was shown more EPS secretion but lower PN and PS total contents under 30 mg L^{-1} of Cu(II), as contrast in Fig. 2A, B. This verified that more cell lysis occurred, leading to more cell lysate, such as nucleic acid and humus, being extracted as EPS (Yu 2020), which was consistent with the 3D-EEM results in Fig. 4. In short, the coping strategy employed by *Bacillus* sp. to alleviate copper stress was as follows: increased Cu(II) stress triggered greater secretion of EPS with a higher PN/PS ratio, resulting in increased cell aggregation and binding with Cu(II) to prevent its entry into cells. The overwhelmingly stimulated secretion of PS over PN indicated a more stable effect of the EPS permeation barrier. However, higher concentrations, i.e., 30 mg L^{-1} of Cu(II) can break through the resistance threshold, causing cell lysis and decreasing the secretion of PS and PN contents.

FTIR and XPS analysis

As shown in Fig. 3A, the peaks at approximately 3300 cm^{-1}, 1070 cm^{-1}, and 540 cm^{-1} displayed the greatest changes under Cu(II) stress. The broad peaks near 3300 cm^{-1} and 1400 cm^{-1} were assigned to the stretching vibration of hydroxyl group (−OH), which may be due to the vibration of amines and/or alcohols in the sugar ring (Yu et al. 2020). However, the overlapping series of vibration in this region made it difficult to accurately determine the changes in functional groups (Fang et al. 2022b). With an increase in Cu(II) concentration from 0 to 30 mg L^{-1}, the two peaks near 1070 cm^{-1} and 540 cm^{-1} were most obviously strengthened in Fig. 3A. This finding indicated an increase in stretching vibration of C−O/C−O−C bond (1070 cm^{-1}) in polysaccharide rings (Zhang et al. 2022) and the in-plane bending vibration of C−C=O bond (540 cm^{-1}) in ketones (Zhang et al. 2021a). These two peaks were recognized as glycosidic linkage (Kang

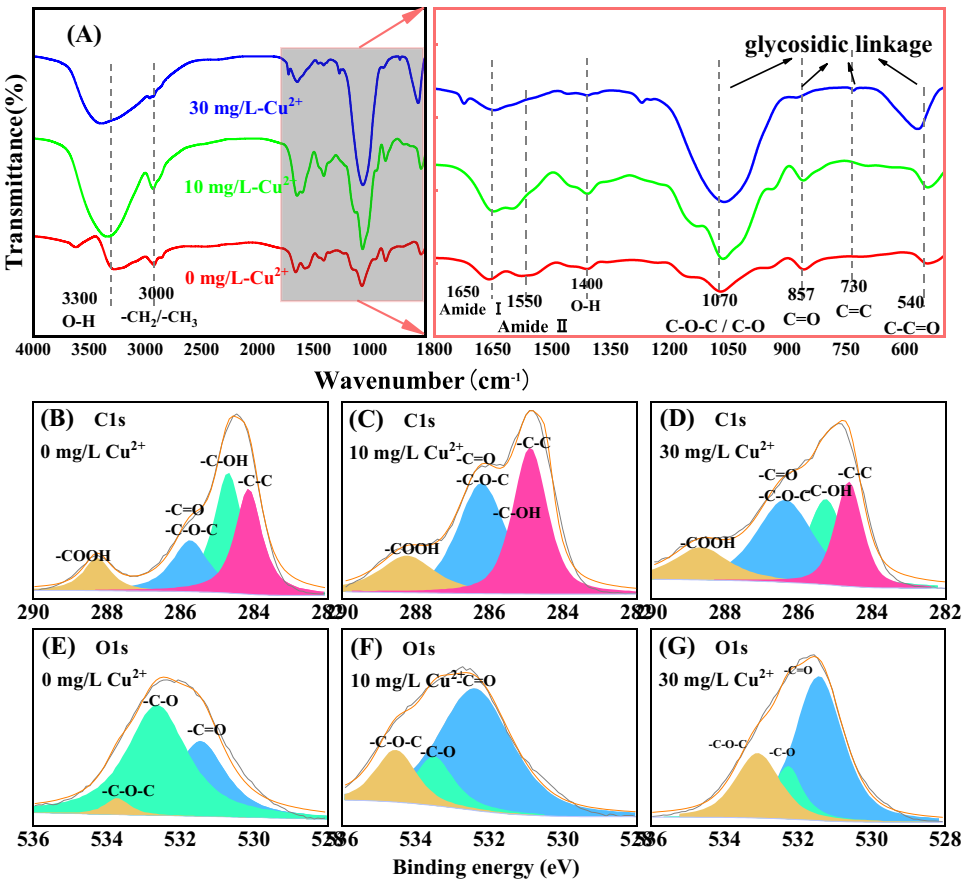

Fig. 3 Fourier-transform infrared (FTIR) spectra of EPS (A) and the XPS analysis of high-resolution peak spectra of C1s (B–D) and O1s (E–G) for EPS extracted from *Bacillus* sp. cultured under initial Cu(II) concentration of 0, 10, and 30 mg L^{-1}

et al. 2014), and the significant enhancement of these two peaks confirmed the results in Fig. 2B, demonstrating that Cu(II) stress could stimulate the secretion of more PS contents to strengthen the EPS effect of permeation barrier.

The high-resolution scans of the C1s and O1s provided in Fig. 3B–G were obtained using EPS. It was observed that the peak intensity at 286.23 eV for C1s and at 533.1 eV and 532.28 eV for O1s changed most obviously with increasing Cu(II) concentrations. After reacting with copper, the intensity of the peak near 286.23 eV showed the most improvement, which was considered as the −C=O or −C−O−C (An et al. 2022). This indicated an increase in carboxylic acid, carboxylate, or amide, which was consistent with the FTIR results as shown in Fig. 3A. This increase may be due to copper stress triggering the secretion of more EPS contents as a protective barrier (Zhang et al. 2021b). Regarding the O1s for EPS, three peak intensities at 533.1 eV, 532.28 eV, and 531.44 were observed and were ascribed to the −C−O−C, −C−O, and −C=O bonds, respectively, which showed different trends with increasing Cu(II) stress. This is consistent with the C1s results, which showed an enhancement of the −C−O−C bond. The variations in the other two peaks may be ascribed to the hydroxyl, carboxyl, and amide groups in PN contents and amino acids (Sha et al. 2022). These observations indicated that the electronic density in the EPS was disturbed by Cu(II) since the three peak intensities showed complementary. In conclusion, the XPS results were consistent well with the FTIR observations, demonstrating an increase in hydroxyl, carboxyl, and amide groups of the EPS under copper stress. The enhancement of these hydrophobic bonds further verified the results in Fig. 2B, which showed an increase in the hydrophobicity of the cell surface under Cu(II) stress. This suggested that the increase in hydrophobicity served as a coping strategy to relieve copper stress.

3D-EEM spectroscopy analysis

Figure 4A–C shows a sharp decrease in peak intensity in four regions (Flu I–III and Flu V) in the EPS. Peak A (Ex/Em 285/350) was assigned to soluble microbial by-product-like substances (SMPs) that were associated with aromatic protein-like substances, such as tyrosine and tryptophan, and could be summarized as PN contents (Zhu et al. 2015) (Qi et al. 2021). Peak A (Ex/Em 285/350) intensity in Flu IV also decreased sharply in the EPS, which may have been due to the combination of tryptophan-like substances with Cu(II) that led to quenching of its fluorescence intensity (Zhang et al. 2021a). Peak B (Ex/Em 350/450) intensity in Flu V weakened the most, indicating the formation of complex substances of copper ions and HS (Zhang et al. 2021b). This is because peak B (Ex/Em 350/450) was associated with fulvic acid-like substances (Bai et al. 2022). Quenching of HS was shown to be attributed to electrostatic interactions between toxic substances and humus through the NH_3^+ and COO^- groups (Yin and Chen 2022), which was consistent with the FTIR results in Fig. 3A that showed an increase in hydroxyl, carboxyl, and amide groups of the EPS under copper stress. This could result in the enhancement of electrostatic interaction between EPS, as demonstrated by Yu (2020) and He et al. (2021).

The differential expression of functional genes

Transcriptome sequencing was used to analyze functional gene changes in *Bacillus* sp. without copper stress (RIN = 9.3) and after exposure to 10 mg L^{-1} of Cu(II) (RIN = 7.2). The gene contrast was carried out using DESeq with the reference gene of *Bacillus altitudinis* (NCBI 66324737), and the contrast rate was high as 94.22%. As shown in Fig. 5A, the circlize package of R language was used to mark differential expression genes, and the volcano map was drawn

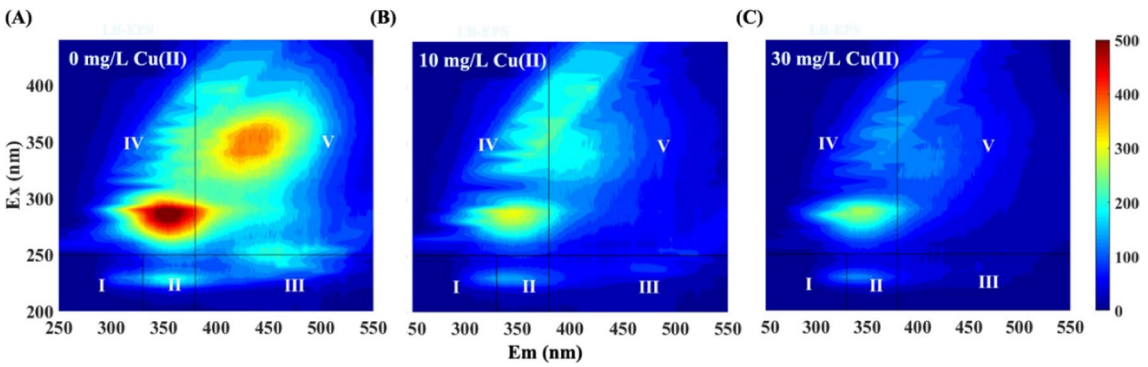

Fig. 4 Three-dimensional excitation-emission matrix (3D-EEM) spectra of EPS extracted under 0, 10, and 30 mg L^{-1} Cu(II) stress (**A**–**C**). And the 3D-EEM spectra were collected with subsequent emission (Em) spectra from 250 to 550 nm at 5 nm increment by varying the excitation (Ex) wavelength from 200 to 500 nm at 5 nm increments. Ex and Em slits were maintained at 5 nm, and the scanning speed was set at 600 nm/min for all the measurements

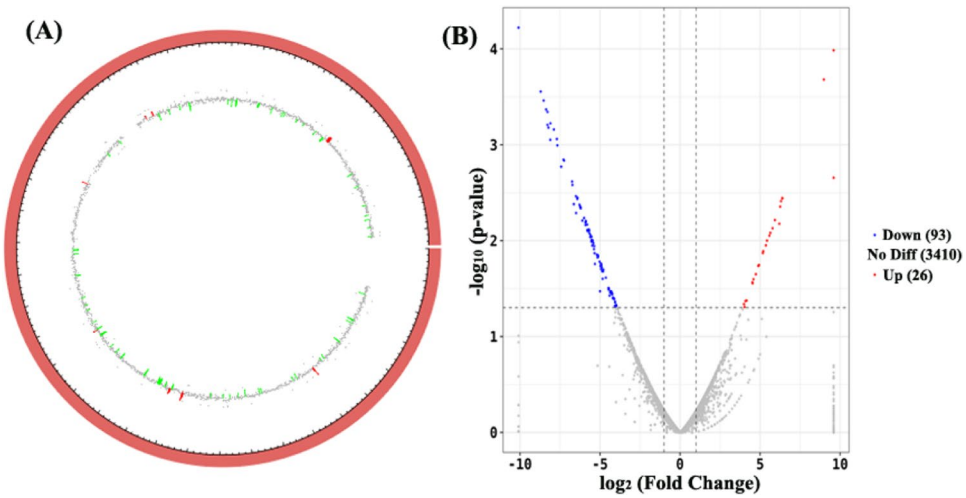

Fig. 5 Comparison of differentially expressed gene amounts for *Bacillus* sp. cultivated under 0 and 10 mg L^{-1} Cu(II) stress. The genome circle map (**A**) and volcano plot of differentially expressed genes (**B**)

using the ggplot2 software package (Fig. 5B). The left side of the volcano map showed the downregulated genes, while the right side showed the upregulated genes compared to the control. The results demonstrated that 26 genes were upregulated, and 93 genes were downregulated in *Bacillus* sp. cultured under 10 mg L^{-1} Cu(II) compared to the blank. The greater number of downregulated genes indicated that the strain activity was inhibited but also initiated the copper resistance mechanism under Cu(II) stress. As shown in the heatmap in Fig. 6A, the two-way clustering analysis using Euclidean method (Guo et al. 2022) clearly divided the differential genes into 9 clusters in Fig. 6B, of which three showed an upward trend, and six showed a downward trend. It demonstrated that the *Bacillus* strain exhibited certain resistance against Cu(II) stress, despite its severe toxicity.

GO and KEGG pathway enrichment analysis

Enrichment analysis was performed on the differentially expressed genes (Xiao et al. 2022). The bubble diagram and histogram of GO enrichment analysis are shown in Fig. 7A, B, respectively. This finding indicated that the biosynthesis of uridine-5′-monophosphate synthase (UMPs) was significantly enhanced, followed by the pyrimidine biosynthesis

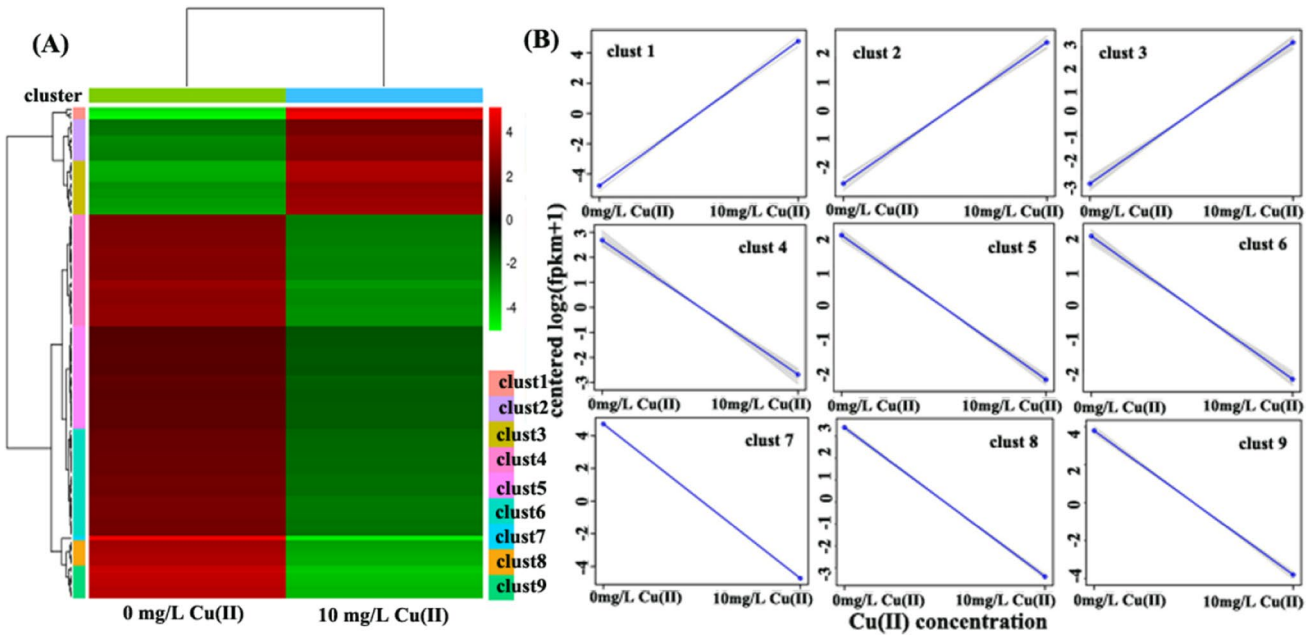

Fig. 6 The heatmap of differentially expressed genes (**A**) and the gene expression trend analysis in each corresponding cluster (**B**) for *Bacillus* sp. cultivated under 0 and 10 mg L^{-1} Cu(II) stress

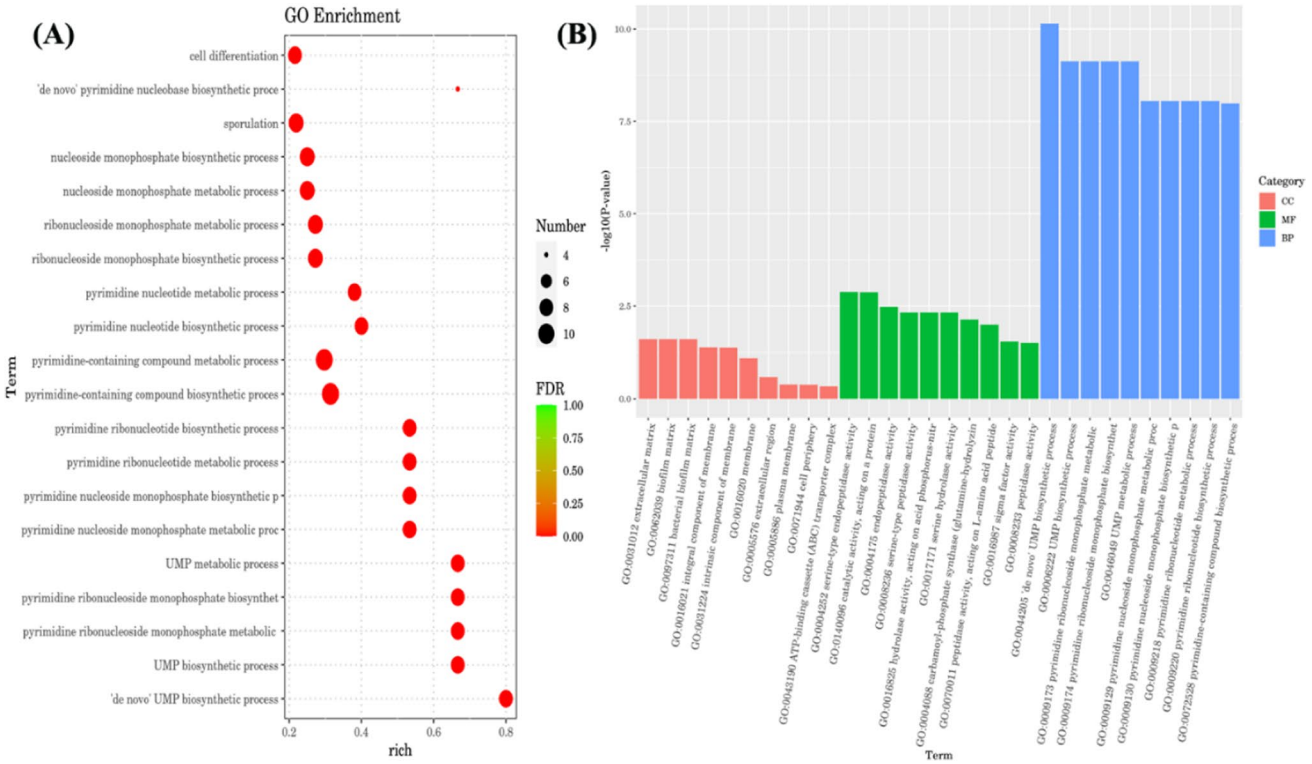

Fig. 7 GO pathway enrichment analysis result comparison of differentially expressed genes for *Bacillus* sp. cultivated under 0 and 10 mg L^{-1} Cu(II) stress. Histogram of GO enrichment analysis (**A**) and the bubble diagram of GO enrichment analysis (**B**)

pathway. The UMP biosynthesis pathway had been shown to enable bacterial cells to sense starvation, nucleic acid degradation, and adapt the production of extracellular matrix to changing environmental conditions (Garavaglia et al. 2012). Interestingly, it has been demonstrated that the adenosine regulatory enzyme, cyclic dimeric guanosine monophosphate (c-di-GMP), played an important role in regulating EPS synthesis (Yu 2020). Therefore, the enhanced UMP biosynthesis pathway served as one of the adenosine regulatory pathways. This pathway was indicated to play a role in EPS regulation resistance mechanisms for cells to adapt to external Cu(II) stress (Wang et al. 2022). The resistance genes enriched in different GO terms could be seen in Table 1, with genes concerning copper ion binding and transport (GO:0005507 and GO0006826) being upregulated. This finding confirmed that copper ions entered the cells and triggered the *Bacillus* sp. strain to improve copper ion binding and transportation, thus verifying that the removal efficiency of 30 mg L^{-1} Cu(II)-containing wastewater was the best, as shown in Fig. 1B.

The upregulation and downregulation of genes enriched in the KEGG pathway are shown in Fig. 8A, B. Three main pathways were found to be enriched for downregulated genes, namely, the secondary metabolic pathway, thiamine metabolic pathway, and C5-branched dibasic acid metabolic pathway. The secondary metabolic pathway was associated with the production of microbial by-products (Fang et al. 2022a). This indicated that the toxicity of Cu(II) suppressed strain activity, which is consistent with the results shown in Fig. 4, where the SMPs in EPS decreased significantly under Cu(II) stress. The thiamine metabolic pathway played a key role in carbohydrate metabolism and the generation of pyruvate and other α-ketoacid coenzyme (Jacobs 2014). The significant downregulation of this pathway indicated that the microbial glucose metabolism was disordered under Cu(II) stress, leading to an increased PN/PS ratio in EPS, as shown in Fig. 2B. The C5-branched dibasic acid metabolic pathway, an essential pathway for microbial electron transport, played an important role in microbial functional metabolism. The downregulation of this pathway indicated that the electron transport capacity of *Bacillus* sp. decreased under Cu(II) toxicity, which was confirmed by the three genes downregulated in Table 2. It was worth noting that cytochromes were recognized as electron transfer substances (Yu 2020), and the downregulation of genes related to cytochrome-mediating enzyme (NM232_RS08855, NM232_RS08860, and NM232_RS18130) indicated a decreased electron transport capacity and oxidative phosphorylation metabolism level of *Bacillus* sp. under Cu(II) stress.

Table 1 Function enrichment analysis results of upregulated genes

GO ID	Term	Ontology	*p* value	FDR
GO:0005507	Copper ion binding	MF	0.0022	0.066
GO:0006825	Copper ion transport	BP	0.021	0.061
GO:0006222	UMP biosynthetic process	BP	1.018*E*−14	3.22*E*−13
GO:0046049	UMP metabolic process	BP	1.018*E*−14	3.22*E*−13
GO:0009218	Pyrimidine ribonucleotide metabolic process	BP	1.30*E*−13	2.29*E*−12
GO:0009220	Pyrimidine ribonucleotide biosynthetic process	BP	1.30*E*−13	2.29*E*−12
GO:0044205	"De novo" UMP biosynthetic process	BP	9.34*E*−16	1.48*E*−13
GO:0004088	Carbamoyl-phosphate synthase (glutamine-hydrolyzing) activity	MF	0.00048	0.048
GO:0016884	Carbon-nitrogen ligase activity, with glutamine as amido-N-donor	MF	0.0079	0.066
GO:0004070	Aspartate carbamoyltransferase activity	MF	0.0092	0.066
GO:0004123	Cystathionine gamma-lyase activity	MF	0.0092	0.066
GO:0004151	Dihydroorotase activity	MF	0.0092	0.066
GO:0004152	Dihydroorotate dehydrogenase activity	MF	0.0092	0.066
GO:0004564	Beta-fructofuranosidase activity	MF	0.0092	0.066
GO:0004588	Orotate phosphoribosyltransferase activity	MF	0.0092	0.066
GO:0004589	Orotate reductase (NADH) activity	MF	0.0092	0.066

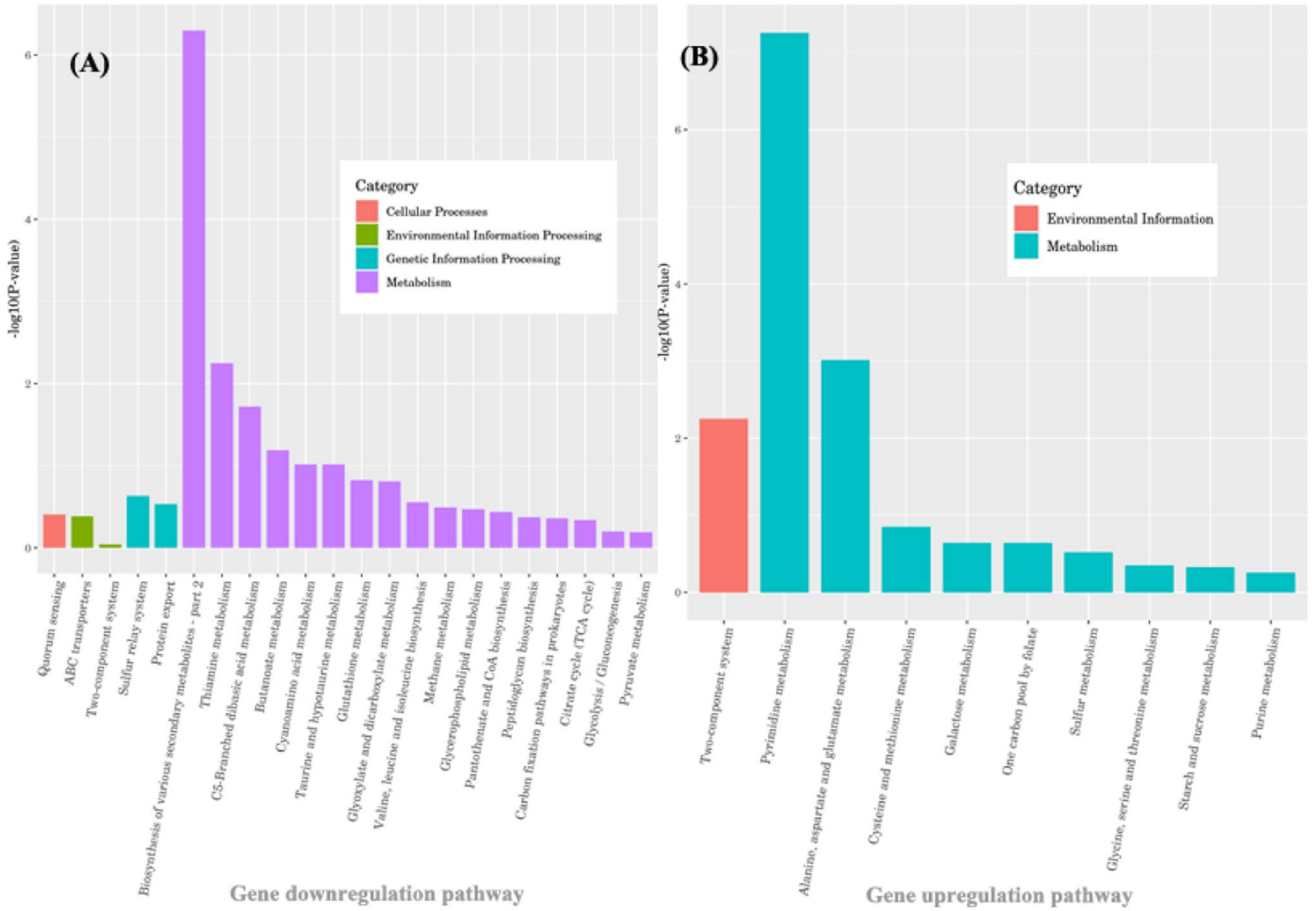

Fig. 8 The KEGG pathway enrichment analysis for of downregulated (**C**) and upregulated (**D**) genes

Table 2 Changes in the expression of copper ion resistance genes

Gene name	NR	Result	Pathway
NM232_RS06790	Heavy metal translocating P-type ATPase	Up	ko04978 (mineral absorption), ko01524 (platinum drug resistance)
NM232_RS08855	Cytochrome aa3 quinol oxidase subunit I	Down	ko00190 (oxidative phosphorylation)
NM232_RS06795	Copper(I) chaperone CopZ, partial	Up	ko04978 (mineral absorption)
NM232_RS06735	Cadmium-translocating P-type ATPase	Up	/
NM232_RS12465	Copper resistance protein CopC	Up	/
NM232_RS06800	Metal-sensing transcriptional repressor	Up	/
NM232_RS17580	Heavy metal translocating P-type ATPase	Up	/
NM232_RS08860	Cytochrome aa3 quinol oxidase subunit II	Down	ko00190 (oxidative phosphorylation)
NM232_RS14055	Multicopper oxidase domain-containing protein	Up	/
NM232_RS18130	Cytochrome c oxidase subunit II	Down	ko00190 (oxidative phosphorylation)

Meanwhile, three KEGG enrichment pathways were significantly upregulated in Fig. 8B: the two-component system (TCS) pathway, the pyrimidine metabolism pathway, and the alanine aspartate and glutamate pathway. The TCS pathway could regulate microbial response to changing environments and facilitate adaptation (Kowluru 2002; Liu et al. 2021). Its significant upregulation indicated that *Bacillus* sp. had initiated an obvious defense mechanism in response to Cu(II) stress. The pyrimidine metabolism played an essential role in the synthesizing polysaccharides, phospholipids, and glycosylating proteins and lipids, leading to the variation of the PS/PN ratio in EPS (Löffler and Zameitat 2013). The alanine aspartate and glutamate pathway was an important pathway in microbial amino acid metabolism, positively correlated with the total antioxidant capacity of cells (Xiao et al. 2022). Its significant upregulation indicated that the redox of amino acid played an important role in the defense mechanism of *Bacillus* sp. under Cu(II) stress. It also confirmed that the PN contents in EPS played an important role in Cu(II) resistance (Wang et al. 2022). Additionally, seven genes related to heavy metal resistance were recognized as upregulated in Table 2, confirming that the strain had established a heavy metal resistance capacity.

Conclusions

In conclusion, this study demonstrated that *Bacillus* sp. could adapt to Cu(II) stress by increasing EPS secretion as a biological self-defense mechanism. The PN/PS ratio of EPS increased with higher Cu(II) stress, and FTIR, XPS, and 3D-EEM spectra showed changes in EPS groups. Cu(II) stress disturbed functional resistance gene expression and metabolic levels, with downregulation of genes related to electron transport and upregulation of genes related to copper ion binding and transport, UMP biosynthesis, pyrimidine metabolism, and TCS pathways. The study suggests that *Bacillus* sp. initiates self-defense mechanisms under Cu(II) stress despite severe cell toxicity, reflected in increased EPS secretion and upregulation of EPS-related genes and metabolic levels.

Author contribution Lingling Wang: investigation, validation, writing—original draft. Zhengyan Yin: investigation, visualization, writing—reviewing and editing. Yun Xu: validation, reviewing, and editing. Miaoyu Deng: methodology, reviewing, and editing. Kaiming Zhang: validation and writing—reviewing and editing. Quan Wang: project administration, reviewing, and editing. Rong-ping Chen: supervision, reviewing, and editing. Lei Yu: project administration, funding acquisition, supervision, reviewing, and editing.

Funding This work was supported by the financial supports of the National Natural Science Foundation of China (Nos. 51778298 and 52200159), the Six Talent Peaks Project of Jiangsu Province (JNHB-052), the Practice and Innovation Training Program Project of College Students (2022NFUSPITP0369), the Natural Science Foundation of Jiangsu Province (BK20220425), the Natural Science Fund for Colleges and Universities in Jiangsu Province (22KJB610016), and the Priority Academic Program Development of Jiangsu Higher Education Institutions (PAPD).

Data availability All data generated or analyzed during this study are included in this paper.

Declarations

Ethical approval and consent to participate Not applicable.

Consent for publication Not applicable.

Competing interests The authors declare no competing interests.

References

An H, Tian T, Wang Z, Jin R, Zhou J (2022) Role of extracellular polymeric substances in the immobilization of hexavalent chromium

by *Shewanella putrefaciens* CN32 unsaturated biofilms. Sci Total Environ 810:151184

Ayangbenro AS, Babalola OO, Aremu OS (2019) Bioflocculant production and heavy metal sorption by metal resistant bacterial isolates from gold mining soil. Chemosphere 231:113–120

Bai X, Liang W, Sun J, Zhao C, Wang P, Zhang Y (2022) Enhanced production of microalgae-originated photosensitizer by integrating photosynthetic electrons extraction and antibiotic induction towards photocatalytic degradation of antibiotic: a novel complementary treatment process for antibiotic removal from effluent of conventional biological wastewater treatment. J Environ Manage 308:114527

Chen Z, Meng Y, Sheng B, Zhou Z, Jin C, Meng F (2019) Linking exoproteome function and structure to anammox biofilm development. Environ Sci Technol 53:1490–1500

Chowdhury S, Mazumder MAJ, Al-Attas O, Husain T (2016) Heavy metals in drinking water: occurrences, implications, and future needs in developing countries. Sci Total Environ 569-570:476–488

Dong Y, Sui M, Jiang Y, Wu J, Wang X (2022) Dibutyl phthalate weakens the role of electroactive biofilm as an efficient wastewater handler and related mechanism. Sci Total Environ 807:151612

Espirito Santo C, Lam EW, Elowsky CG, Quaranta D, Domaille DW, Chang CJ, Grass G (2011) Bacterial killing by dry metallic copper surfaces. Appl Environ Microbiol 77:794–802

Fang L, Wei X, Cai P, Huang Q, Chen H, Liang W, Rong X (2011) Role of extracellular polymeric substances in Cu(II) adsorption on Bacillus subtilis and Pseudomonas putida. Bioresour Technol 102:1137–1141

Fang S, Qin T, Yu T, Zhang G (2022a) Improvement of the gut microbiota in vivo by a short-chain fatty acids-producing strain *Lactococcus garvieae* CF11. Processes 10

Fang X, Sun S, Liao X, Li S, Zhou S, Gan Q, Zeng L, Guan Z (2022b) Effect of diurnal temperature range on bioleaching of sulfide ore by an artificial microbial consortium. Sci Total Environ 806:150234

Fu JJ, Huang DQ, Bai YH, Shen YY, Lin XZ, Huang Y, Ling YR, Fan NS, Jin RC (2022) How anammox process resists the multi-antibiotic stress: resistance gene accumulation and microbial community evolution. Sci Total Environ 807:150784

Garavaglia M, Rossi E, Landini P (2012) The pyrimidine nucleotide biosynthetic pathway modulates production of biofilm determinants in *Escherichia coli*. PLoS One 7:e31252

Guo A, Zhou Q, Bao Y, Qian F, Zhou X (2022) Prochloraz alone or in combination with nano-CuO promotes the conjugative transfer of antibiotic resistance genes between *Escherichia coli* in pure water. J Hazard Mater 424:127761

Hashim MA, Mukhopadhyay S, Sahu JN, Sengupta B (2011) Remediation technologies for heavy metal contaminated groundwater. J Environ Manage 92:2355–2388

He T, Hua JQ, Chen RP, Yu L (2021) Adsorption characteristics of methylene blue by a dye-degrading and extracellular polymeric substance -producing strain. J Environ Manage 288:112446

Holmes AH, Moore LSP, Sundsfjord A, Steinbakk M, Regmi S, Karkey A, Guerin PJ, Piddock LJV (2016) Understanding the mechanisms and drivers of antimicrobial resistance. The Lancet 387:176–187

Hua JQ, Zhang R, Chen RP, Liu GX, Yin K, Yu L (2021) Energy-saving preparation of a bioflocculant under high-salt condition by using strain *Bacillus* sp. and the interaction mechanism towards heavy metals. Chemosphere 267:129324

Jacobs M (2014) Thiamine. Encyclopedia of Toxicology:537–538

Jamshidifard S, Koushkbaghi S, Hosseini S, Rezaei S, Karamipour A, Jafari Rad A, Irani M (2019) Incorporation of UiO-66-NH2 MOF into the PAN/chitosan nanofibers for adsorption and membrane filtration of Pb(II), Cd(II) and Cr(VI) ions from aqueous solutions. J Hazard Mater 368:10–20

Kang F, Alvarez PJ, Zhu D (2014) Microbial extracellular polymeric substances reduce Ag^+ to silver nanoparticles and antagonize bactericidal activity. Environ Sci Technol 48:316–322

Kang F, Qu X, Alvarez PJ, Zhu D (2017) Extracellular saccharide-mediated reduction of Au(3+) to gold nanoparticles: new insights for heavy metals biomineralization on microbial surfaces. Environ Sci Technol 51:2776–2785

Kowluru A (2002) Identification and characterization of a novel protein histidine kinase in the islet beta cell: evidence for its regulation by mastoparan, an activator of G-proteins and insulin secretion. Biochem Pharmacol 63:2091–2100

Li GF, Ma WJ, Ren ZQ, Wang Y, Li JP, Zhao JW, Li ST, Liu Q, Gu YN, Cheng YF, Huang BC, Jin RC (2021) Molecular insight into the binding property and mechanism of sulfamethoxazole to extracellular proteins of anammox sludge. Environ Sci Technol 55:16627–16635

Li Q, Song W, Sun M, Li J, Yu Z (2020) Response of *Bacillus vallismortis* sp. EPS to exogenous sulfur stress/ induction and its adsorption performance on Cu(II). Chemosphere 251:126343

Li YP, You LX, Yang XJ, Yu YS, Zhang HT, Yang B, Chorover J, Feng RW, Rensing C (2022) Extrapolymeric substances (EPS) in *Mucilaginibacter rubeus* P2 displayed efficient metal(loid) bio-adsorption and production was induced by copper and zinc. Chemosphere 291:132712

Lian Z, Yang Z, Song W, Sun M, Gan Y, Bai X (2022) Effects of different exogenous cadmium compounds on the chemical composition and adsorption properties of two gram-negative bacterial EPS. Sci Total Environ 806:150511

Liu L, Xu S, Wang F, Yan Z, Tian Z, Ji M (2021) Effect of exogenous N-acyl-homoserine lactones on the anammox process at 15: nitrogen removal performance, gene expression and metagenomics analysis. Bioresour Technol 341:125760

Löffler M, Zameitat E (2013) Pyrimidine biosynthesis and degradation (catabolism). Encyclopedia Biol Chem:712–718

Ma XL, He EJ, Cao FT, Fan YY, Zhou XT, Xiao X (2022) Re-evaluation of the environmental hazards of nZnO to denitrification: performance and mechanism. Chemosphere 291:132824

Meis JE, Khanna A (2009) RNA amplification and cDNA synthesis for qRT-PCR directly from a single cell. Nat Methods 6:an12-an13

Mohd Nasir N, Mohd Yunos FH, Wan Jusoh HH, Mohammad A, Lam SS, Jusoh A (2019) Subtopic: advances in water and wastewater treatment harvesting of Chlorella sp. microalgae using *Aspergillus niger* as bio-flocculant for aquaculture wastewater treatment. J Environ Manage 249:109373

Ola ATT, Heryanto H, Armynah B, Tahir D (2023) Bibliometric analysis of chitosan research for wastewater treatment: a review. Environ Monit Assess 195:474–474

Qi P, Li T, Hu C, Li Z, Bi Z, Chen Y, Zhou H, Su Z, Li X, Xing X (2021) Effects of cast iron pipe corrosion on nitrogenous disinfection by-products formation in drinking water distribution systems via interaction among iron particles, biofilms, and chlorine. Chemosphere 292:133364

Sha L, Wu Z, Ling Z, Liu X, Yu X, Zhang S (2022) Investigation on the improvement of activated sludge dewaterability using different iron forms (ZVI vs. Fe(II))/peroxydisulfate combined vertical electro-dewatering processes. Chemosphere 292:133416

Tang R, Luo H, Prommer H, Yue Z, Wang W, Su K, Hu ZH (2021) Response of anaerobic granular sludge to long-term loading of roxarsone: from macro- to micro-scale perspective. Water Res 204:117599

Vale G, Mehennaoui K, Cambier S, Libralato G, Jomini S, Domingos RF (2016) Manufactured nanoparticles in the aquatic environment-biochemical responses on freshwater organisms: a critical overview. Aquat Toxicol 170:162–174

Van Acker H, Van Dijck P, Coenye T (2014) Molecular mechanisms of antimicrobial tolerance and resistance in bacterial and fungal biofilms. Trends Microbiol 22:326–333

Vasudevan S, Oturan MA (2013) Electrochemistry: as cause and cure in water pollution—an overview. Environ Chem Lett 12:97–108

Wang L, Yuan L, Li ZH, Zhang X, Leung KMY, Sheng GP (2022) Extracellular polymeric substances (EPS) associated extracellular antibiotic resistance genes in activated sludge along the AAO process: distribution and microbial secretors. Sci Total Environ 816:151575

Wang ZY, Ju CJ, Zhang R, Hua JQ, Chen RP, Liu GX, Yin K, Yu L (2021) Acceleration of the bio-reduction of methyl orange by a magnetic and extracellular polymeric substance nanocomposite. J Hazard Mater 420:126576

Weber O, Scholz RW, Buhlmann R, Grasmuck D (2001) Risk perception of heavy metal soil contamination and attitudes toward decontamination strategies. Risk analysis : an official publication of the Society for Risk Analysis 21:967–977

Xia PF, Li Q, Tan LR, Sun XF, Song C, Wang SG (2016) Extracellular polymeric substances protect *Escherichia coli* from organic solvents. Rsc Adv 6:59438–59444

Xiao Y, Zhang YM, Xu WB, Chen DY, Li BW, Cheng YX, Guo XL, Dong WR, Shu MA (2022) The effects of salinities stress on histopathological changes, serum biochemical index, non-specific immune and transcriptome analysis in red swamp crayfish *Procambarus clarkii*. Sci Total Environ 840:156502

Xu J, Cao Z, Zhang Y, Yuan Z, Lou Z, Xu X, Wang X (2018) A review of functionalized carbon nanotubes and graphene for heavy metal adsorption from water: preparation, application, and mechanism. Chemosphere 195:351–364

Yi Q, Wu S, Southam G, Robertson L, You F, Liu Y, Wang S, Saha N, Webb R, Wykes J, Chan TS, Lu YR, Huang L (2021) Acidophilic iron- and sulfur-oxidizing bacteria, acidithiobacillus ferrooxidans, drives alkaline pH neutralization and mineral weathering in Fe ore tailings. Environ Sci Technol 55:8020–8034

Yin M, Chen H (2022) Unveiling the dual faces of chitosan in anaerobic digestion of waste activated sludge. Bioresour Technol 344:126182

Yu HQ (2020) Molecular insights into extracellular polymeric substances in activated sludge. Environ Sci Technol 54:7742–7750

Yu L, Hua JQ, Fan HC, George O, Lu Y (2020) Simultaneous nitriles degradation and bioflocculant production by immobilized *K. oxytoca* strain in a continuous flow reactor. J Hazard Mater 387:121697

Zhang J, Peng Y, Li X, Du R (2022) Feasibility of partial-denitrification/ anammox for pharmaceutical wastewater treatment in a hybrid biofilm reactor. Water Res 208:117856

Zhang L, Ye L, Yin Z, Xiao K, Jing C (2021a) Mechanistic study of antimonate reduction by *Escherichia coli* W3110. Environ Pollut 291:118258

Zhang R, Chang ZY, Wang LL, Cheng WX, Chen RP, Yu L, Qiu XH, Han JG (2021b) Solid-liquid separation of real cellulose- containing wastewaters by extracellular polymeric substances: mechanism and cost evaluation. Sep Purif Technol 279:119665

Zhao Y, Gao J, Zhang W, Wang Z, Cui Y, Dai H, Li D, Zhang Y (2022) Robustness of the partial nitrification-anammox system exposing to triclosan wastewater: stress relieved by extracellular polymeric substances and resistance genes. Environ Res 206:112606

Zheng Y, Fang X, Ye Z, Li Y, Cai W (2008) Biosorption of Cu(II) on extracellular polymers from *Bacillus* sp. F19. J Environ Sci 20:1288–1293

Zhu L, Zhou J, Lv M, Yu H, Zhao H, Xu X (2015) Specific component comparison of extracellular polymeric substances (EPS) in flocs and granular sludge using EEM and SDS-PAGE. Chemosphere 121:26–32